Cardiomyocyte-Specific Overexpression of Human Stem Cell Factor Improves Cardiac Function and Survival After Myocardial Infarction in Mice

Fu-Li Xiang, MD; Xiangru Lu, MD; Lamis Hammoud, PhD; Ping Zhu, MD, PhD; Peter Chidiac, PhD; Jeffrey Robbins, PhD; Qingping Feng, MD, PhD

Background—Soluble stem cell factor (SCF) has been shown to mobilize bone marrow stem cells and improve cardiac repair after myocardial infarction (MI). However, the effect of membrane-associated SCF on cardiac remodeling after MI is not known. The present study investigated the effects of cardiomyocyte-specific overexpression of the membrane-associated isoform of human SCF (hSCF) on cardiac function after MI.

Methods and Results—A novel mouse model with tetracycline-inducible and cardiac-specific overexpression of membrane-associated hSCF was generated. MI was induced by left coronary artery ligation. Thirty-day mortality after MI was decreased in hSCF/tetracycline transactivator (tTA) compared with wild-type mice. In vivo cardiac function was significantly improved in hSCF/tTA mice at 5 and 30 days after MI compared with wild-type mice. Endothelial progenitor cell recruitment and capillary density were increased and myocardial apoptosis was decreased in the peri-infarct area of hSCF/tTA mice. Myocyte size was decreased in hSCF/tTA mice 30 days after MI compared with WT mice. Furthermore, hSCF overexpression promoted de novo angiogenesis as assessed by matrigel implantation into the left ventricular myocardium.

Conclusions—Cardiomyocyte-specific overexpression of hSCF improves myocardial function and survival after MI. These beneficial effects of hSCF may result from increases in endothelial progenitor cell recruitment and neovascularization and decreases in myocardial apoptosis and cardiac remodeling. **(*Circulation*. 2009;120:1065-1074.)**

Key Words: angiogenesis ■ apoptosis ■ heart failure ■ myocardial infarction ■ remodeling ■ stem cell factor

Myocardial infarction (MI) is responsible for about one third of heart failure cases and causes ≈2 million deaths per year worldwide.[1] MI leads to scar formation and subsequent ventricular remodeling, which is characterized by infarct expansion, progressive fibrous replacement of myocardium, hypertrophic growth of the noninfarct myocardium, and left ventricular (LV) dilatation. Cardiac remodeling contributes to the development of heart failure after MI.[2] Despite optimal pharmacological treatment, the prognosis of heart failure remains poor.[3]

Clinical Perspective on p 1074

Stem cell factor (SCF), also known as Steel factor, mast cell growth factor, or *c-kit* ligand, binds to its receptor *c-kit* and promotes survival, proliferation, mobilization, and adhesion of all *c-kit*–expressing cells, which includes hematopoietic stem cells, endothelial progenitor cells,[4,5] and cardiac stem cells.[6] SCF is expressed as a glycosylated transmembrane protein by many cells and tissues, including stromal cells, fibroblasts, endothelium, and myocardium.[7,8] Alternative splicing leads to 2 isoforms of SCF: soluble and membrane-associated (SCF) isoforms, which differ in the absence or presence of a proteolytic cleavage site encoded by exon 6. Soluble SCF and membrane-associated SCF have distinct but overlapping roles. Membrane-associated SCF, the dominant isoform in vivo, induces a more persistent receptor activation and is more effective at promoting long-term support of target cell survival.[9] Transgene expression of membrane-associated SCF in Steel-dickie (*sld*) mutant mice resulted in a significant relief from anemia and bone marrow hypoplasia.[10] In contrast, overexpression of the full-length soluble form of the SCF transgene had no effect on red blood

Received November 26, 2008; accepted July 10, 2009.

From the Departments of Physiology and Pharmacology (F.-L.X., L.H., P.C., Q.F.), and Medicine (Q.F.), University of Western Ontario, and Lawson Health Research Institute (X.L., Q.F.), London, Ontario, Canada; Department of Cardiovascular Surgery, Guangdong Cardiovascular Institute, Guangdong General Hospital, and Guangdong Academy of Medical Sciences, Guangzhou, China (P.Z.); and Department of Pediatrics, Division of Molecular Cardiovascular Biology, Children's Hospital Research Foundation, Cincinnati, Ohio (J.R.).

The online-only Data Supplement is available with this article at http://circ.ahajournals.org/cgi/content/full/CIRCULATIONAHA.108.839068/DC1.

Correspondence to Dr Qingping Feng, Department of Physiology and Pharmacology, University of Western Ontario, London, Ontario, Canada N6A 5C1. E-mail qfeng@uwo.ca

Circulation **is available at http://circ.ahajournals.org** **DOI: 10.1161/CIRCULATIONAHA.108.839068**

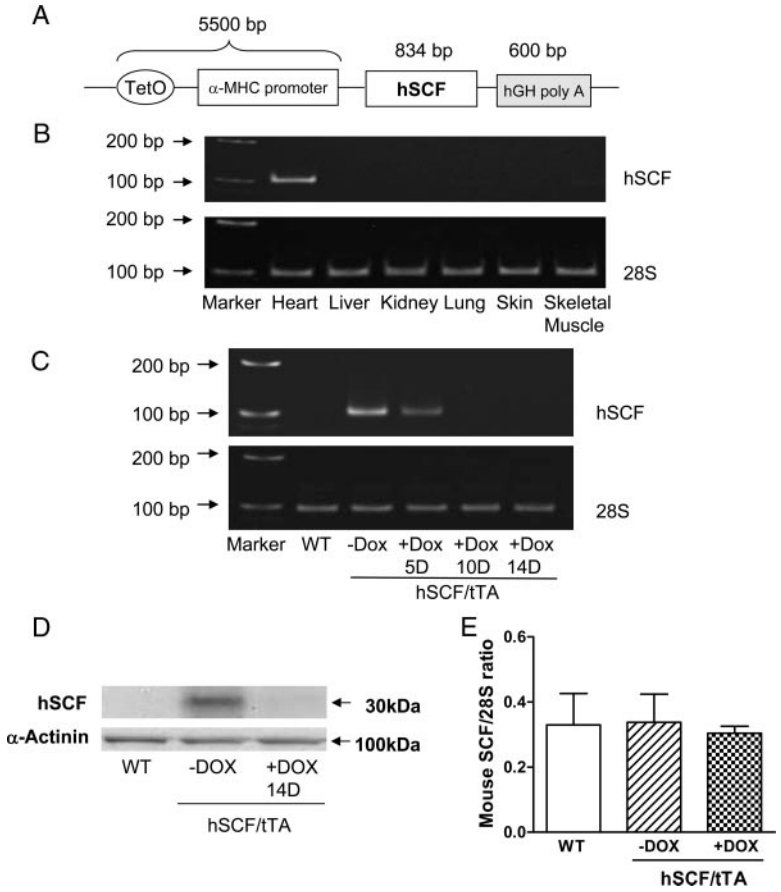

Figure 1. Generation and characterization of the inducible hSCF/tTA transgenic mouse. A, Illustration of the membrane-associated hSCF transgenic constructs used to create the hSCF transgenic mice. B, Expression of hSCF mRNA was detected in the heart but not in other organs of hSCF/tTA mice in the absence of DOX. C, Cardiac expression of hSCF mRNA in hSCF/tTA mice after treatment with DOX for 5, 10, and 14 days. D, Protein expression of human SCF in heart tissue was measured by Western blotting. Human SCF protein was expressed exclusively in hSCF/tTA-DOX mice. E, Endogenous mouse SCF mRNA expression determined by real-time PCR was not significantly altered among WT, hSCF/tTA-DOX, and hSCF/tTA+DOX mice. Data are mean±SEM; n=5 to 7 per group. One-way ANOVA followed by Bonferroni test.

cell production but corrected the myeloid progenitor cell deficiency seen in these mutants.[10] Recently, treatment with soluble SCF in combination with granulocyte-colony stimulating factor improved cardiac repair and survival after MI, whereas soluble SCF treatment alone did not.[11] Because the membrane-associated SCF has a much different biological profile compared with soluble SCF, it is possible that cardiac-specific overexpression of membrane-associated SCF may promote cardiac repair mechanisms after MI.

We hypothesized that inducible cardiomyocyte-specific overexpression of membrane-associated human SCF (hSCF) could improve cardiac repair, myocardial function, and survival after MI. To test this hypothesis, we generated a novel transgenic mouse that overexpresses membrane-associated hSCF in cardiomyocytes under the control of a Tet-off system.[12] We demonstrated that cardiomyocyte-specific hSCF overexpression increased myocardial neovascularization, decreased ventricular remodeling, and increased survival after MI. Our study suggests a novel therapeutic potential of hSCF in the treatment of heart failure after MI.

Methods

Generation of hSCF/Tetracycline Transactivator Double-Transgenic Mice

Animals in this study were handled in accordance with the *Guide for the Care and Use of Laboratory Animals* published by the US National Institutes of Health (NIH publication No. 85–23, revised 1996). A new line of tetracycline-inducible cardiac-specific mice overexpressing hSCF was generated. Briefly, membrane-associated hSCF complementary DNA (accession No. NM_003994) was inserted into the inducible α-myosin heavy chain promoter expression vector to permit doxycycline (DOX)-regulated expression in combination with a cardiac-specific tetracycline transactivator (tTA)–expressing transgene. The hSCF mice were crossed with cardiac-specific tTA mice previously created[12] to produce wild-type (WT), tTA, hSCF, and hSCF/tTA mice. To turn off hSCF expression, the hSCF/tTA mice were treated with 0.2 mg/mL DOX in their drinking water for 2 weeks before until 5 or 30 days after sham or MI surgery.

Supplemental Methodology

For a detailed explanation of methods relative to generation of hSCF/tTA double-transgenic mice, real-time reverse-transcriptase polymerase chain reaction (RT-PCR), induction of MI, infarct size measurement,[13] histological and hemodynamic analyses,[14,15] measurements of apoptosis,[16] in vivo matrigel angiogenesis,[15] and statistical analysis, please see the Material section of the online-only Data Supplement.

Results

Generation and Characterization of the Conditional Cardiac-Specific hSCF/tTA Double-Transgenic Mice

hSCF mice were generated with the hSCF transgene expression under the control of a tetracycline-responsive element containing the α-myosin heavy chain promoter (Figure 1A). The hSCF transgenic mice were then crossed with cardiac-specific tTA mice to generate the inducible cardiac-specific hSCF/tTA double-transgenic mice. The resulting offspring

Table 1. General Information on Control and hSCF/tTA Mice Subjected to Sham or MI Surgery

	Sham		MI	
Parameters	Controls	hSCF/tTA	Controls	hSCF/tTA
n	24	21	81	66
Age at surgery, d	85±4	83±6	83±3	86±3
Sex, M/F	24/0	21/0	68/13	56/10
Body weight, g	27.8±0.9	26.0±0.8	26.6±0.6	26.5±0.6
Infarct size, % of LV	. . .	. . .	38.6±0.8	38.5±0.7

Data are mean±SEM and analyzed by 2-way ANOVA with Bonferroni test for age, sex, and body weight. Infarct size was compared by Student *t* test. There was no statistical difference between control and hSCF/tTA mice in any of the parameters listed within the sham or MI groups. Controls include WT, tTA, and hSCF mice. Total number of animals includes all 5- and 30-day groups and the DOX treatment groups.

were genotyped by PCR with both tTA and hSCF primers. Cardiac-specific expression of hSCF was verified by RT-PCR. Expression of hSCF can be detected in the heart tissue but not in liver, kidney, skin, lung, or skeletal muscle (Figure 1B). The inducible expression of hSCF in cardiomyocytes was verified with both RT-PCR and Western blot techniques. Results showed that a high level of hSCF mRNA and protein expression was observed in the hearts of hSCF/tTA mice in the absence of DOX. After 10 to 14 days of continuous DOX administration, the expression of hSCF in hSCF/tTA mice was abrogated at both the mRNA and protein levels (Figure 1C and 1D). Transgene expression did not affect endogenous mouse SCF expression because myocardial mouse SCF mRNA levels analyzed with real-time RT-PCR were similar among WT, hSCF/tTA-DOX, and hSCF/tTA+DOX mice (Figure 1E). Furthermore, there were no coat color changes in any of the hSCF/tTA mice.

Post-MI SCF Expression

A total of 87 hSCF/tTA mice and 105 littermates (tTA, hSCF, and WT) were subjected to coronary artery ligation or sham operation. General characteristics of these animals are shown in Table 1. There were no statistical differences in age, sex, or body weight between hSCF/tTA mice and littermates in the sham or MI groups (*P*=NS). Protein expression of mouse SCF after MI was studied by Western blot analysis in WT mice. Myocardial mouse SCF protein levels were significantly decreased at 5 days ($P<0.05$; Figure 2A) but not at 30 days (*P*=NS; Figure 2B) after MI compared with the sham group. The expression of hSCF as determined by real-time RT-PCR in hSCF/tTA mice was unchanged in the peri-infarct area at 5 days (Figure 2C) and 30 days (Figure 2D) after MI compared with shams.

Survival and Cardiac Function After MI

Postoperation survival was monitored for 30 days in the WT and hSCF/tTA sham groups and in the WT and hSCF/tTA MI groups (n=13, 11, 37, and 34, respectively). Survival of the sham groups was 100%. MI resulted in significantly lower survival compared with the sham groups ($P<0.05$). However, the 30-day survival of hSCF/tTA MI mice was significantly higher compared with WT mice (85% versus 54%; $P<0.01$; Figure 3A).

To evaluate the effect of cardiac-specific hSCF expression on cardiac function, LV hemodynamic parameters were analyzed by a pressure-volume analysis system 5 and 30 days after MI. There was no significant difference in heart rate, mean arterial pressure, or cardiac output between hSCF/tTA and littermate controls (Tables 2 and 3). Five days after MI, cardiac function of WT MI mice as determined by LV dP/dt, −dP/dt, and preload-adjusted maximum power was significantly decreased compared with sham groups ($P<0.05$, Figure 3B). In the absence of DOX, which expresses hSCF, LV dP/dt, −dP/dt, and preload-adjusted maximum power were significantly restored in hSCF/tTA MI mice (hSCF/tTA MI versus WT MI, $P<0.05$; Figure 3B). The increase in cardiac function was completely blocked by DOX treatment, which turned off hSCF expression (hSCF/tTA+DOX MI

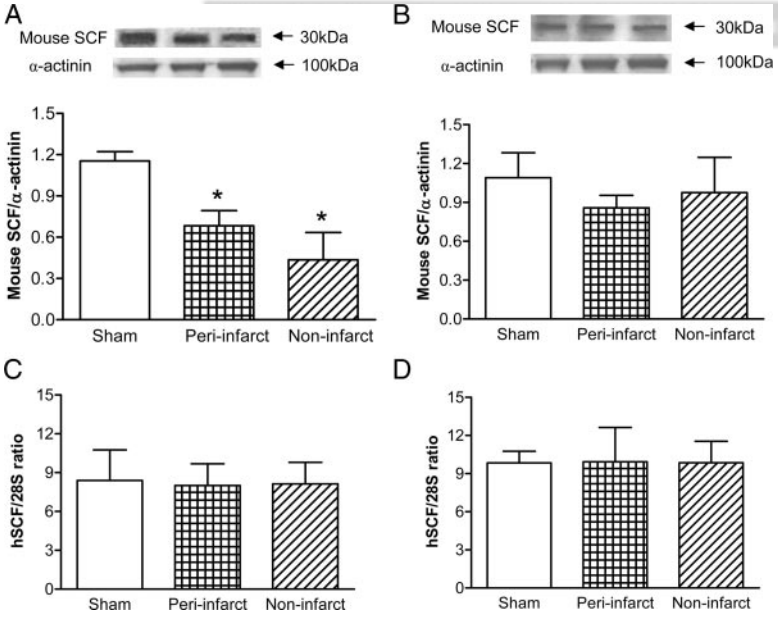

Figure 2. Mouse SCF expression in the heart after MI. Myocardial mouse SCF protein levels at 5 days (A) and 30 days (B) after MI were measured by Western blot analysis in WT mice. Compared with the sham group, mouse SCF protein levels were significantly decreased at 5 but not 30 days after MI. hSCF mRNA expression was detected in hSCF/tTA mice at 5 days (C) and 30 days (D) after MI by real-time RT-PCR. There was no significant change in cardiac hSCF expression in hSCF/tTA mice after MI. Data are mean±SEM; n=4 to 5 per group. One-way ANOVA followed by Bonferroni test: *$P<0.05$ vs sham.

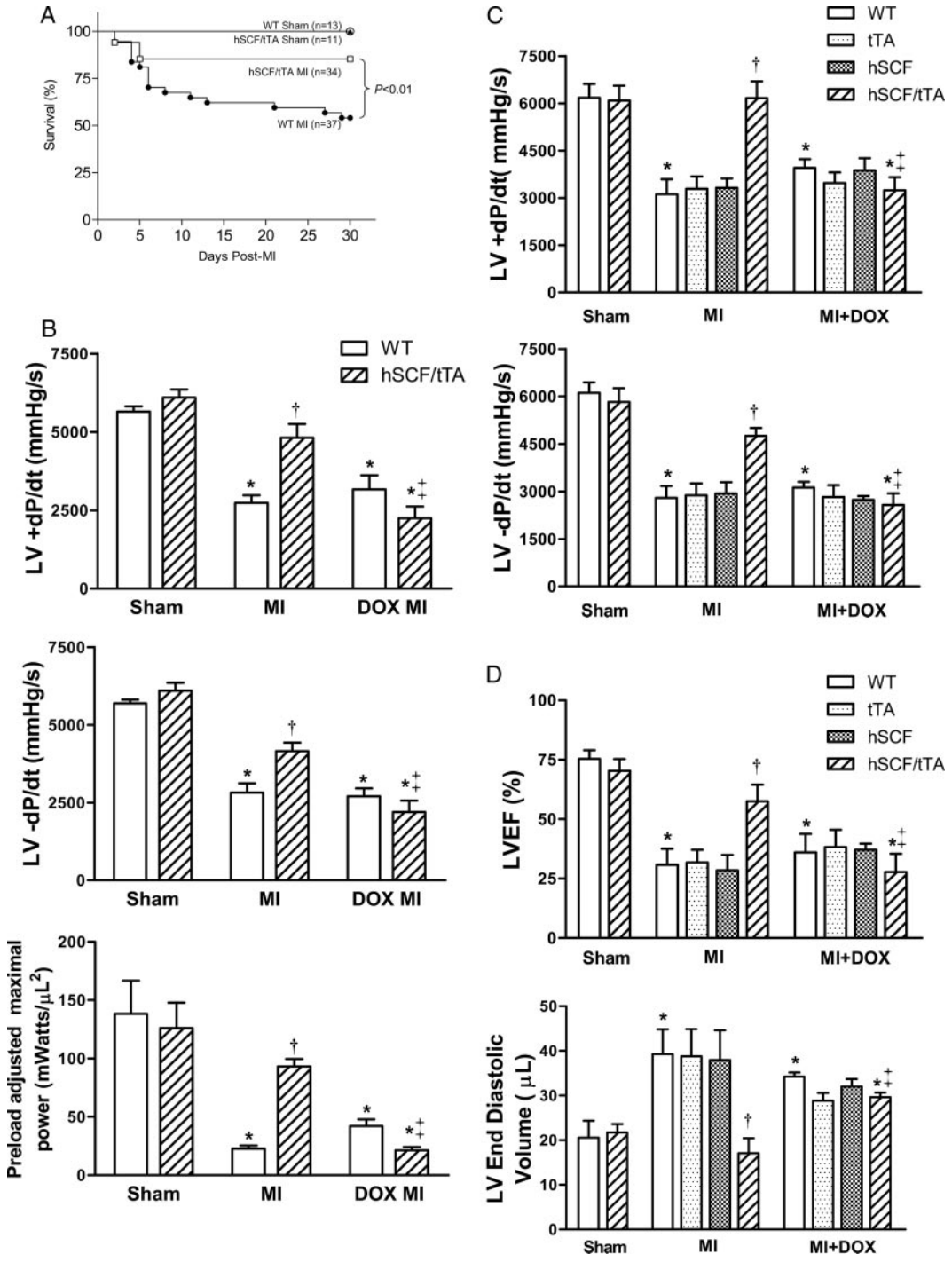

Figure 3. Survival and LV function after MI. A, Survival was monitored for 30 days after MI in WT sham, hSCF/tTA sham, WT MI, and hSCF/tTA MI mice. Mortality was significantly decreased in the hSCF/tTA MI group vs WT MI (log-rank test with Bonferroni corrections). B, Changes in LV dP/dt and preload-adjusted maximum power 5 days after MI. The hSCF/tTA MI group presented a significantly better LV function compared with WT MI. The improvement was abrogated in the hSCF/tTA+DOX group. C and D, Changes in LV dP/dt, ejection fraction (LVEF), and LV end-diastolic volume 30 days after MI. Both systolic and diastolic functions were significantly improved in hSCF/tTA MI mice, which were abrogated by DOX treatment. B through D, Data are mean±SEM; n=5 to 8 per group. Two-way ANOVA followed by Bonferroni test: *$P<0.05$ vs sham groups; †$P<0.01$ vs WT MI; ‡$P<0.05$ vs hSCF/tTA-DOX MI.

versus hSCF/tTA MI, $P<0.05$; Figure 3B). Thirty days after surgery, LV dP/dt, −dP/dt, and ejection fraction were significantly decreased in WT, tTA, and hSCF MI groups compared with WT shams ($P<0.05$; Figure 3C and 3D). Overexpression of hSCF significantly improved cardiac function (hSCF/tTA MI versus WT, tTA, and hSCF MI groups, $P<0.05$; Figure 3C and 3D). Furthermore, LV end-diastolic volume was significantly increased in the WT, tTA, and hSCF MI groups compared with WT shams but significantly decreased in hSCF/tTA MI mice compared with other MI

Table 2. Hemodynamic Parameters of WT and hSCF/tTA Mice 5 Days After MI

Parameters	WT	hSCF/tTA	*P*
n	6	5	
Heart rate, bpm	362±26	354±20	0.82
MAP, mm Hg	93±6	90±8	0.88
LVEF, %	23±4	40±3	0.01
SW, mW	171±35	441±111	0.07
CO, μL/min	2087±293	3089±628	0.20
PAMP, mW/mL^2	31±9	75±10	0.008

MAP indicates mean artery pressure; LVEF, LV ejection fraction; SW, stroke work; CO, cardiac output; and PAMP, preload-adjusted maximum power. Data are mean±SEM and analyzed by unpaired Student *t* test.

groups ($P<0.05$; Figure 3D). However, the improvement in cardiac function in hSCF/tTA mice 30 days after MI was abrogated after DOX treatment (Figure 3C and 3D).

Myocardial Apoptosis 5 Days After MI

To investigate mechanisms responsible for the improvement in cardiac function by cardiac-specific hSCF overexpression, myocardial apoptosis in the peri-infarct area was studied 5 days after MI. Myocardial apoptosis was determined by caspase-3 activity and cell-death ELISA. Both caspase-3 activity and cytosolic DNA fragments were significantly increased in the WT MI group compared with the sham group ($P<0.05$), whereas these indexes were significantly decreased in the hSCF/tTA MI mice compared with the WT MI group ($P<0.05$; Figure 4A and 4B). The decrease in apoptosis was abrogated in the hSCF/tTA+DOX MI group in which the expression of hSCF was turned off ($P<0.05$; Figure 4A and 4B).

Stem Cell Recruitment and Growth Factor Release After MI

Stem cell recruitment to the peri-infarct area of the myocardium was evaluated by *c-kit* and *c-kit*/vascular endothelial

Table 3. Hemodynamic Parameters of Control and hSCF/tTA Mice 30 Days After MI

Parameters	WT	tTA	hSCF	hSCF/tTA	*P*
n	6	5	5	6	
Heart rate, bpm	326±25	323±12	311±29	318±21	0.97
MAP, mm Hg	87±5	83±8	76±7	85±5	0.63
LVEF, %	31±7	32±5	28±7	58±7	0.0149
SW, mW	438±219	509±150	409±114	700±298	0.77
Cardiac output, μL/min	4052±1302	3895±744	3635±1134	4027±867	0.99
PAMP, mW/mL^2	24±4	38±15	46±25	212±45	0.0003

Abbreviations as in Table 2. Data are mean±SEM and analyzed by 1-way ANOVA followed by Bonferroni test, with $P<0.017$ indicating statistical significance. *P* values (unadjusted) are comparisons between WT and hSCF/tTA mice.

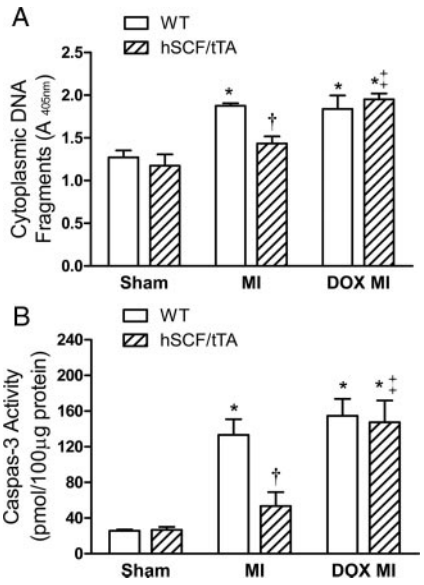

Figure 4. Myocardial apoptosis in peri-infarct area 5 days after MI. Expression of hSCF in hSCF/tTA-DOX MI mice significantly reduced apoptosis as measured by caspase-3 activity (A) and cell-death ELISA (B). These effects were abrogated by turning off the expression of hSCF in hSCF/tTA+DOX MI mice. Data are mean±SEM; n=5 to 8. Two-way ANOVA followed by Bonferroni test: *$P<0.05$ vs sham; †$P<0.05$ vs WT MI; ‡$P<0.05$ vs hSCF/tTA-DOX MI.

growth factor (VEGF) receptor 2 (VEGFR2) double staining. Because VEGFR2 is an important marker for endothelial progenitor cells (EPCs), cells positive for *c-kit*/VEGFR2 are likely EPCs. Representative fluorescent photomicrographs at 5 and 30 days after MI are shown in Figure 5A and 5C. Quantitative analysis showed that there were significantly more *c-kit*$^+$ and *c-kit*$^+$/VEGFR2$^+$ cells retained in the peri-infarct area in hSCF/tTA compared with WT mice 5 days after MI ($P<0.05$; Figure 5C). Treatment with DOX, which turns off hSCF expression, abrogated the recruitment of *c-kit*$^+$ and *c-kit*$^+$/VEGFR2$^+$ cells ($P<0.05$; Figure 5C). Interestingly, 80% of the cells were *c-kit*$^+$/VEGFR2$^+$, indicating that the majority of stem cells are EPCs. Furthermore, capillaries in the peri-infarct area were positive for *c-kit* and VEGFR2 in the hSCF/tTA mice (Figure 5A, third panel), suggesting incorporation of EPCs into the newly formed vessels. At 30 days after MI, myocardial stem cell density in the peri-infarct area was decreased to similar low levels in both WT and hSCF/tTA mice (Figure 5C and 5D).

Mast cells also express *c-kit*. To analyze myocardial mast cell density, heart sections were stained with toluidine blue. Consistent with previous studies, there were very few mast cells in shams or infarct myocardium in WT mice,[17] and no significant increase in mast cells was observed in hSCF/tTA mice at either 5 or 30 days after MI (see Table I and Figure I of the online-only Data Supplement). Thus, the influence of mast cells on *c-kit*$^+$ stem cell analysis in the infarct myocardium is negligible in the present study.

Previous studies have implicated growth factors, including VEGF-A, insulin growth factor-1, and basic fibroblast growth factor, in cardiac repair after MI.[18] To determine the expression of these growth factors, real-time RT-PCR was used.

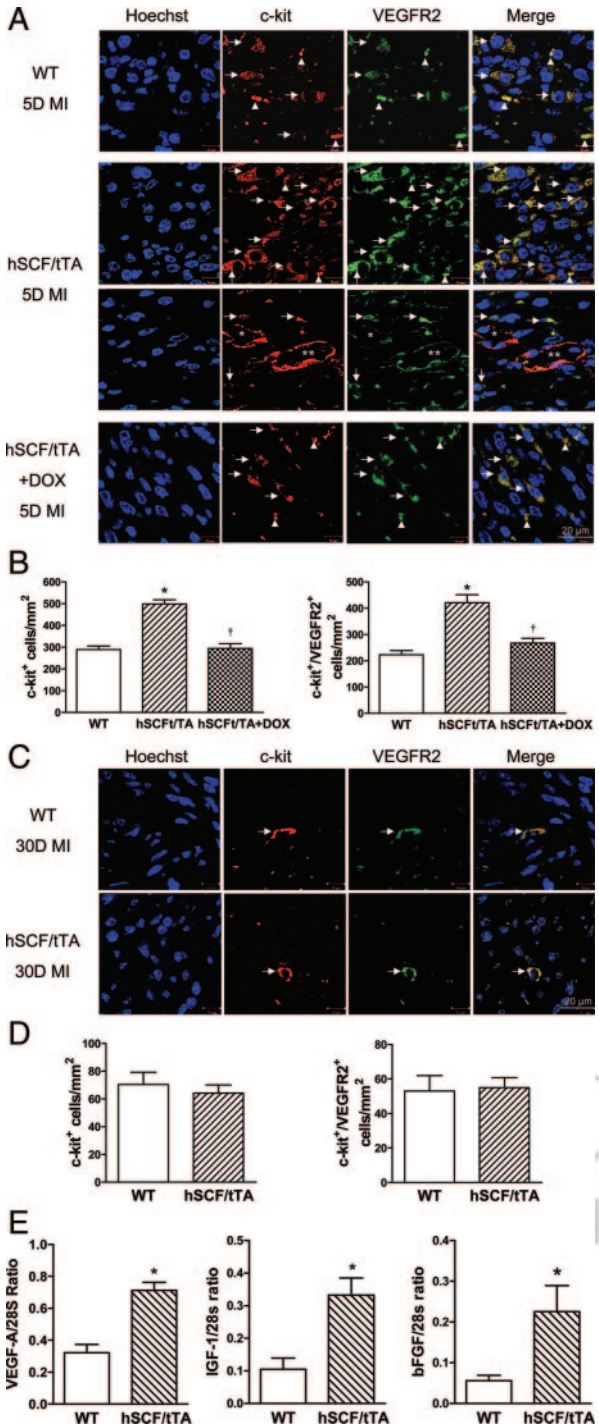

Figure 5. *c-kit*$^+$ and *c-kit*$^+$/VEGFR2$^+$ cells retained and growth factors released in the peri-infarct area after MI. A and C, Representative confocal images of Hoechst (blue; nuclei), *c-kit* (red), and VEGFR2 (green) staining 5 and 30 days after MI. Panel 3 in A shows a capillary positive for *c-kit* (*) and a capillary positive for both c-kit and VEGFR2 (**) in hSCF/tTA mice 5 days after MI. Arrows indicate positive signals; arrowheads, red blood cells. B, Quantitative analysis of *c-kit*$^+$ and *c-kit*$^+$/VEGFR2$^+$ cells in the peri-infarct area 5 days after MI. D, Quantitative analysis of *c-kit*$^+$ and *c-kit*$^+$/VEGFR2$^+$ cells in the peri-infarct area 30 days after MI. E, Myocardial VEGF-A, insulin growth factor-1 (IGF-1), and basic fibroblast growth factor (bFGF) mRNA determined by real-time RT-PCR 5 days after MI. Data are mean±SEM; n=5 to 8. B, One-way ANOVA followed by Bonferroni test: *$P<0.05$ vs WT MI; †$P<0.05$ vs hSCF/tTA-DOX MI. E, Unpaired Student *t* test: *$P<0.05$ vs WT.

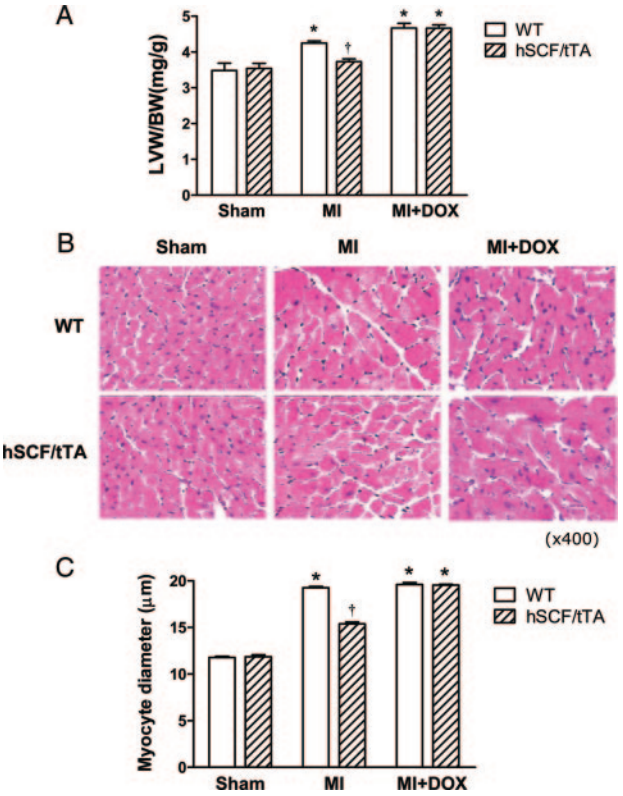

Figure 6. LV hypertrophy 30 days after MI. A, Ratios of LV to body weight 30 days after MI or sham operations. B, Representative photomicrographs of hematoxylin and eosin–stained sections showing the cross sections of cardiomyocytes. C, Quantitative analysis of myocyte diameters in WT and hSCF/tTA mice after sham and MI surgeries in the presence or absence of DOX. Data are mean±SEM; n=5 to 11. Two-way ANOVA followed by Bonferroni test: *$P<0.05$ vs sham groups; †$P<0.05$ vs WT MI.

The mRNA levels of VEGF-A, insulin growth factor-1, and basic fibroblast growth factor in the peri-infarct area 5 days after MI were significantly increased in hSCF/tTA compared with WT mice ($P<0.05$; Figure 5E).

LV Hypertrophy 30 Days After MI

The ratio of LV weight to body weight, a measure of LV hypertrophy, was similar between sham groups but was significantly increased in WT MI mice compared with WT shams ($P<0.05$; Figure 6A). However, the ratio in hSCF/tTA MI mice was significantly decreased compared with WT MI mice ($P<0.05$, Figure 6A). MI-induced LV hypertrophy was further studied at the cellular level by histological analysis. Representative photomicrographs of hematoxylin and eosin stained sections are shown in Figure 6B. Myocyte transverse diameters were assessed using the minimum cross-sectional diameter at the nuclear level to reduce the effects of myocyte orientation on cell size measurements.[19] The minimum cross-sectional diameter was similar between sham groups but was significantly increased in the WT MI compared with WT sham mice ($P<0.05$; Figure 6C). However, the hSCF/tTA MI mice showed significantly smaller myocyte cross-sectional diameters compared with those of WT MI mice ($P<0.05$; Figure 6C). Furthermore, these effects were abrogated when

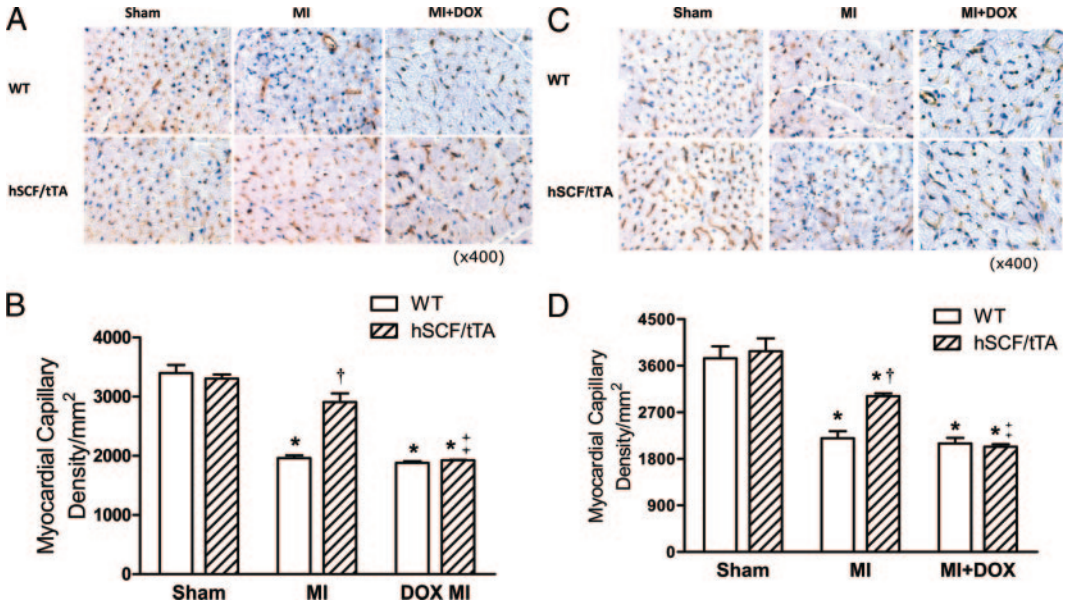

Figure 7. Myocardial capillary density after MI. Capillaries were identified by endothelial specific lectin-I staining at 5 days (A and B) and 30 days (C and D) after MI in WT, hSCF/tTA, and hSCF/tTA+DOX mice. A and C, Representative photomicrographs of lectin-I–stained sections from each experiment group showing individual capillaries (brown staining). Nuclei were stained by hematoxylin. B and D, Quantitative analysis of capillary density. Data are mean±SEM; n=5 to 6 per group. Two-way ANOVA followed by Bonferroni test: *$P<0.05$ vs sham; †$P<0.05$ vs WT MI; ‡$P<0.05$ vs hSCF/tTA MI.

hSCF expression was turned off by DOX treatment (Figure 6A and 6C).

Capillary Density After MI

To quantify myocardial capillary density, lectin-I staining was used to specifically stain endothelial cells. Representative photomicrographs of lectin-I staining are presented in Figure 7A (5 days after MI) and Figure 7C (30 days after MI). In mice 5 days after surgery, myocardial capillary density was similar between WT and hSCF/tTA sham mice (Figure 7B). The capillary density in the peri-infarct area of the MI group was significantly decreased compared with the sham groups ($P<0.05$; Figure 7B). When hSCF expression was activated in the hSCF/tTA mice in the absence of DOX, capillary density was significantly increased (hSCF/tTA MI versus WT MI, $P<0.05$; Figure 7B). However, the increase was abrogated by DOX treatment in hSCF/tTA mice (hSCF/tTA+DOX MI versus hSCF/tTA MI, $P<0.05$; Figure 7B). Capillary density also was assessed 30 days after surgery. Myocardial capillary density was similar between WT and hSCF/tTA sham mice (Figure 7D). Capillary density in the peri-infarct area of the MI groups was significantly decreased compared with the respective sham groups ($P<0.05$; Figure 7D). Overexpression of hSCF significantly increased capillary density (hSCF/tTA MI versus WT MI, $P<0.05$; Figure 7D). DOX treatment abrogated the increase in capillary density in hSCF/tTA mice (Figure 7D).

In Vivo Myocardial Angiogenesis

The ability of the hSCF expressed in the cardiomyocytes to promote angiogenesis was investigated in vivo by implanting matrigel into the LV myocardium for 3 days. As shown in Figure 8A, the matrigel was surrounded by inflammatory cells and could be easily identified in the myocardium. The newly formed vessels that penetrated into the gel plug showed aneurysm-like structures inside the gel. The area of capillaries and aneurysm-like structures penetrating the matrigel plug was quantified in relation to the total matrigel area. The percentage of vessel-like areas was significantly increased in hSCF/tTA compared with WT mice ($P<0.05$; Figure 8B).

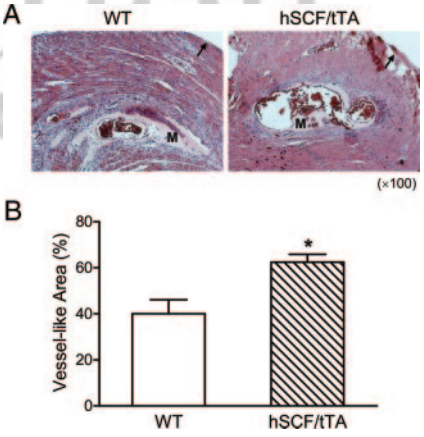

Figure 8. Myocardial angiogenesis WT and hSCF/tTA mice. Matrigel (M) was implanted into the LV myocardium for 3 days. A, Representative images of hematoxylin and eosin–stained heart sections. The lumens and the aneurysm-like structures are the newly formed vessels, which have grown into the matrigel. Arrows indicate epicardium. B, Quantitative analysis of angiogenesis. The area of capillary-like structures in relation to the total matrigel area was quantified and expressed as percent vessel-like area. Data are mean±SEM from 6 mice per group. Unpaired Student *t* test: *$P<0.05$ vs WT group.

Discussion

The present study demonstrates for the first time that cardiomyocyte-specific expression of membrane-associated hSCF improves survival and cardiac function after MI. The beneficial effects of transgene expression are associated with reduced myocardial apoptosis, increased recruitment of stem cells to the infarcted myocardium, enhanced myocardial neovascularization, and attenuated ventricular remodeling. The improvements in cardiac function and myocardial angiogenesis are a result of hSCF overexpression because treatment with DOX, which turns off hSCF expression, abrogates these effects after MI. Our study suggests that hSCF may have therapeutic potential in the treatment of heart failure after MI.

C-kit signaling can promote cardiac repair after MI. Administration of *c-kit*$^+$ stem cells, whether through intravenous injection or local delivery into the infarcted myocardium after MI, improves cardiac function, enhances angiogenesis, and impairs cardiac remodeling.[20,21] On the other hand, *c-kit*–deficient (*W/W*^{v}) mice exhibit dilated cardiomyopathy after MI. After replacement with normal WT bone marrow, the cardiomyopathic phenotype of *W/W*^{v} mice is rescued.[22,23] However, the *W/W*^{v} mice have defects in hematopoietic stem cell function, abnormal islet β-cell development, and impaired glucose tolerance.[24,25] These abnormalities also likely contribute to the impaired cardiac repair after MI. As the ligand of *c-kit*, soluble SCF is increased in the bone marrow after myocardial ischemia/reperfusion injury, leading to EPC mobilization and improvement in myocardial neovascularization and cardiac function.[26] Furthermore, peri-infarct injections of soluble SCF increased *c-kit*$^+$ stem cell recruitment to the infarcted heart after intravenous administration of bone marrow–derived stem cells.[27] Although this effect lasted 72 hours, no functional benefit was observed.

After MI, circulating *c-kit*$^+$ bone marrow stem cells and EPCs are increased.[28–30] However, stem cell attractants SDF-1 and SCF, and proangiogenic genes such as VEGF-A and VEGFR2 are decreased in the infarct region after MI.[8] The stem/progenitor cells mobilized into the peripheral blood may not be recruited in sufficient numbers or retained in the infarcted myocardium to participate in cardiac repair because of decreased myocardial expression of stem cell attractants such as SCF.[8]

To increase the recruitment and retention of stem/progenitor cells in the infarcted myocardium and to improve cardiac repair after MI, we generated a cardiomyocyte-specific membrane-associated hSCF-overexpressing mouse. Although our findings imply enhanced signaling, endogenous SCF expression and signaling were previously found to be reduced in mice strongly overexpressing hSCF starting from embryonic development in multiple tissues under the control of human phosphoglycerate kinase promoter.[31] This was interpreted as evidence that hSCF antagonizes mouse SCF signaling.[31] However, studies have shown that hSCF behaves as a full agonist at mouse *c-kit*.[32,33] It follows that strong hSCF overexpression may desensitize and/or downregulate $\geq$1 key components of mouse *c-kit* signaling, consistent with the observed loss of endogenous SCF.[31] Our mouse model differs from the one in the previous study in that a relatively weak cardiac-specific promoter was used to induce hSCF expression only postnatally, and thus endogenous mouse SCF downregulation and "functional antagonism" were not observed.

Our data showed that cardiac-specific overexpression of hSCF promoted EPC recruitment to the infarcted myocardium. Importantly, these cells participated in the angiogenic process in that they were incorporated into the newly formed vessels in the infarcted myocardium. Consistent with this hypothesis, myocardial capillary density was increased in the hSCF-overexpressing mice after MI. In addition, *c-kit* signaling can increase cell survival and stem cell function.[34,35] Thus, although the absolute number of stem cells retained in the infarcted myocardium is only doubled by hSCF overexpression, it is possible that the improvement in survival and functional capacity of these stem cells could result in the increased release of soluble factors, causing beneficial paracrine actions in the myocardium.[18] In support of this paracrine hypothesis, expression of several candidate mediators such as VEGF-A, basic fibroblast growth factor, and insulin growth factor-1 was increased in the myocardium overexpressing membrane-associated hSCF after MI. Indeed, hSCF overexpression decreases myocardial apoptosis and cardiac hypertrophy, leading to improvement in cardiac function and survival after MI.

Effects of SCF on cardiac function also have been studied through the use of cardiac transplantation of mesenchymal stem cells transfected with a full-length mouse SCF complementary DNA plasmid expressing both soluble and membrane-associated SCF.[36] Transplantation of mesenchymal stem cells containing SCF plasmids enhanced EPC recruitment and myocardial angiogenesis after MI for $\approx$2 weeks. However, there was no change in animal survival among all treatment groups. Furthermore, cardiac function determined at 4 weeks after MI was not significantly improved by SCF transfection compared with the mesenchymal stem cell group.[36] This is not surprising because >95% of the transplanted mesenchymal stem cells are cleared within 7 days after transplantation into the myocardium.[37] In the present study, to study the long-term effects of SCF on the infarcted myocardium, we chose to express the membrane-associated isoform of hSCF specifically in the heart. hSCF expressed on the membrane of cardiomyocytes serves as a chemoattractant for circulating stem cells to migrate to and stay in the myocardium. hSCF expression was stable and sustained over the entire study period. Furthermore, the Tet-off system used allowed reversible cardiac expression of hSCF. In this regard, treatment with DOX turned off hSCF expression and reversed the beneficial effects of hSCF in mice with MI. Our data showed that cardiomyocyte-specific hSCF overexpression promoted angiogenesis, increased capillary density, decreased myocardial apoptosis, and reduced LV hypertrophy after MI. These beneficial effects led to significant improvements in cardiac function and survival in hSCF/tTA mice after MI and are likely due to the enhanced recruitment and retention of EPCs to the infarct myocardium and improved cardiac repair. Cardiac regeneration via transdifferentiation from bone marrow stem cells in vivo after MI is still debatable.[20] Whether hSCF overexpression promotes

myocardial regeneration from resident cardiac stem cells requires further investigation.

Sources of Funding

This study was supported by grants from the Heart and Stroke Foundation of Ontario (T-6040 to Dr Feng) and the Canadian Institutes of Health Research (MOP-64395 to Dr Feng). Dr Feng is a Heart and Stroke Foundation of Ontario Career Investigator.

Disclosures

None.

References

1. Rosamond W, Flegal K, Furie K, Go A, Greenlund K, Haase N, Hailpern SM, Ho M, Howard V, Kissela B, Kittner S, Lloyd-Jones D, McDermott M, Meigs J, Moy C, Nichol G, O'Donnell C, Roger V, Sorlie P, Steinberger J, Thom T, Wilson M, Hong Y. Heart disease and stroke statistics—2008 update: a report from the American Heart Association Statistics Committee and Stroke Statistics Subcommittee. *Circulation*. 2008;117:e25–e146.
2. Sutton MG, Sharpe N. Left ventricular remodeling after myocardial infarction: pathophysiology and therapy. *Circulation*. 2000;101:2981–2988.
3. Thomas S, Rich MW. Epidemiology, pathophysiology, and prognosis of heart failure in the elderly. *Heart Fail Clin*. 2007;3:381–387.
4. Smith MA, Court EL, Smith JG. Stem cell factor: laboratory and clinical aspects. *Blood Rev*. 2001;15:191–197.
5. Asahara T, Murohara T, Sullivan A, Silver M, van der Zee R, Li T, Witzenbichler B, Schatteman G, Isner JM. Isolation of putative progenitor endothelial cells for angiogenesis. *Science*. 1997;275:964–967.
6. Beltrami AP, Barlucchi L, Torella D, Baker M, Limana F, Chimenti S, Kasahara H, Rota M, Musso E, Urbanek K, Leri A, Kajstura J, Nadal-Ginard B, Anversa P. Adult cardiac stem cells are multipotent and support myocardial regeneration. *Cell*. 2003;114:763–776.
7. Heinrich MC, Dooley DC, Freed AC, Band L, Hoatlin ME, Keeble WW, Peters ST, Silvey KV, Ey FS, Kabat D. Constitutive expression of steel factor gene by human stromal cells. *Blood*. 1993;82:771–783.
8. Vandervelde S, van Luyn MJ, Rozenbaum MH, Petersen AH, Tio RA, Harmsen MC. Stem cell-related cardiac gene expression early after murine myocardial infarction. *Cardiovasc Res*. 2007;73:783–793.
9. Miyazawa K, Williams DA, Gotoh A, Nishimaki J, Broxmeyer HE, Toyama K. Membrane-bound Steel factor induces more persistent tyrosine kinase activation and longer life span of c-kit gene-encoded protein than its soluble form. *Blood*. 1995;85:641–649.
10. Kapur R, Majumdar M, Xiao X, McAndrews-Hill M, Schindler K, Williams DA. Signaling through the interaction of membrane-restricted stem cell factor and c-kit receptor tyrosine kinase: genetic evidence for a differential role in erythropoiesis. *Blood*. 1998;91:879–889.
11. Ohtsuka M, Takano H, Zou Y, Toko H, Akazawa H, Qin Y, Suzuki M, Hasegawa H, Nakaya H, Komuro I. Cytokine therapy prevents left ventricular remodeling and dysfunction after myocardial infarction through neovascularization. *FASEB J*. 2004;18:851–853.
12. Sanbe A, Gulick J, Hanks MC, Liang Q, Osinska H, Robbins J. Reengineering inducible cardiac-specific transgenesis with an attenuated myosin heavy chain promoter. *Circ Res*. 2003;92:609–616.
13. Feng Q, Lu X, Jones DL, Shen J, Arnold JMO. Increased inducible nitric oxide synthase expression contributes to myocardial dysfunction and higher mortality post-myocardial infarction in mice. *Circulation*. 2001;104:700–704.
14. Peng T, Zhang T, Lu X, Feng Q. JNK1/c-fos inhibits cardiomyocyte TNF-alpha expression via a negative crosstalk with ERK and p38 MAPK in endotoxaemia. *Cardiovasc Res*. 2009;81:733–741.
15. Zhao X, Lu X, Feng Q. Deficiency in endothelial nitric oxide synthase impairs myocardial angiogenesis. *Am J Physiol Heart Circ Physiol*. 2002;283:H2371–H2378.
16. Feng Q, Song W, Lu X, Hamilton JA, Lei M, Peng T, Yee SP. Development of heart failure and congenital septal defects in mice lacking endothelial nitric oxide synthase. *Circulation*. 2002;106:873–879.
17. Dewald O, Ren G, Duerr GD, Zoerlein M, Klemm C, Gersch C, Tincey S, Michael LH, Entman ML, Frangogiannis NG. Of mice and dogs: species-specific differences in the inflammatory response following myocardial infarction. *Am J Pathol*. 2004;164:665–677.
18. Gnecchi M, He H, Noiseux N, Liang OD, Zhang L, Morello F, Mu H, Melo LG, Pratt RE, Ingwall JS, Dzau VJ. Evidence supporting paracrine hypothesis for Akt-modified mesenchymal stem cell-mediated cardiac protection and functional improvement. *FASEB J*. 2006;20:661–669.
19. Scherrer-Crosbie M, Ullrich R, Bloch KD, Nakajima H, Nasseri B, Aretz HT, Lindsey ML, Vancon AC, Huang PL, Lee RT, Zapol WM, Picard MH. Endothelial nitric oxide synthase limits left ventricular remodeling after myocardial infarction in mice. *Circulation*. 2001;104:1286–1291.
20. Murry CE, Reinecke H, Pabon LM. Regeneration gaps: observations on stem cells and cardiac repair. *J Am Coll Cardiol*. 2006;47:1777–1785.
21. Nesselmann C, Ma N, Bieback K, Wagner W, Ho A, Konttinen YT, Zhang H, Hinescu ME, Steinhoff G. Mesenchymal stem cells and cardiac repair. *J Cell Mol Med*. 2008;12:1795–1810.
22. Fazel S, Cimini M, Chen L, Li S, Angoulvant D, Fedak P, Verma S, Weisel RD, Keating A, Li RK. Cardioprotective c-kit$^+$ cells are from the bone marrow and regulate the myocardial balance of angiogenic cytokines. *J Clin Invest*. 2006;116:1865–1877.
23. Ayach BB, Yoshimitsu M, Dawood F, Sun M, Arab S, Chen M, Higuchi K, Siatskas C, Lee P, Lim H, Zhang J, Cukerman E, Stanford WL, Medin JA, Liu PP. Stem cell factor receptor induces progenitor and natural killer cell-mediated cardiac survival and repair after myocardial infarction. *Proc Natl Acad Sci U S A*. 2006;103:2304–2309.
24. Sharma Y, Astle CM, Harrison DE. Heterozygous kit mutants with little or no apparent anemia exhibit large defects in overall hematopoietic stem cell function. *Exp Hematol*. 2007;35:214–220.
25. Krishnamurthy M, Ayazi F, Li J, Lyttle AW, Woods M, Wu Y, Yee SP, Wang R. c-Kit in early onset of diabetes: a morphological and functional analysis of pancreatic beta-cells in c-KitW-v mutant mice. *Endocrinology*. 2007;148:5520–5530.
26. Fazel SS, Chen L, Angoulvant D, Li SH, Weisel RD, Keating A, Li RK. Activation of c-kit is necessary for mobilization of reparative bone marrow progenitor cells in response to cardiac injury. *FASEB J*. 2008;22:930–940.
27. Lutz M, Rosenberg M, Kiessling F, Eckstein V, Heger T, Krebs J, Ho AD, Katus HA, Frey N. Local injection of stem cell factor (SCF) improves myocardial homing of systemically delivered c-kit$^+$ bone marrow-derived stem cells. *Cardiovasc Res*. 2008;77:143–150.
28. Leone AM, Rutella S, Bonanno G, Abbate A, Rebuzzi AG, Giovannini S, Lombardi M, Galiuto L, Liuzzo G, Andreotti F, Lanza GA, Contemi AM, Leone G, Crea F. Mobilization of bone marrow-derived stem cells after myocardial infarction and left ventricular function. *Eur Heart J*. 2005;26:1196–1204.
29. Massa M, Rosti V, Ferrario M, Campanelli R, Ramajoli I, Rosso R, De Ferrari GM, Ferlini M, Goffredo L, Bertoletti A, Klersy C, Pecci A, Moratti R, Tavazzi L. Increased circulating hematopoietic and endothelial progenitor cells in the early phase of acute myocardial infarction. *Blood*. 2005;105:199–206.
30. Wojakowski W, Tendera M, Michalowska A, Majka M, Kucia M, Maslankiewicz K, Wyderka R, Ochala A, Ratajczak MZ. Mobilization of CD34/CXCR4$^+$, CD34/CD117$^+$, c-met$^+$ stem cells, and mononuclear cells expressing early cardiac, muscle, and endothelial markers into peripheral blood in patients with acute myocardial infarction. *Circulation*. 2004;110:3213–3220.
31. Kapur R, Everett ET, Uffman J, McAndrews-Hill M, Cooper R, Ryder J, Vik T, Williams DA. Overexpression of human stem cell factor impairs melanocyte, mast cell, and thymocyte development: a role for receptor tyrosine kinase-mediated mitogen activated protein kinase activation in cell differentiation. *Blood*. 1997;90:3018–3026.
32. Lev S, Yarden Y, Givol D. Dimerization and activation of the kit receptor by monovalent and bivalent binding of the stem cell factor. *J Biol Chem*. 1992;267:15970–15977.
33. Martin FH, Suggs SV, Langley KE, Lu HS, Ting J, Okino KH, Morris CF, McNiece IK, Jacobsen FW, Mendiaz EA, Birkett NC, Smith KA, Johnson MJ, Parker VP, Flores JC, Patel AC, Fisher EF, Erjavec HO, Herrera CJ, Wypych J, Sachdev RK, Pope JA, Leslie I, Wen D, Lin CH, Cupples RL, Zsebo KM. Primary structure and functional expression of rat and human stem cell factor DNAs. *Cell*. 1990;63:203–211.
34. Ogawa M, Matsuzaki Y, Nishikawa S, Hayashi S, Kunisada T, Sudo T, Kina T, Nakauchi H. Expression and function of c-kit in hemopoietic progenitor cells. *J Exp Med*. 1991;174:63–71.
35. Edling CE, Hallberg B. c-Kit-a hematopoietic cell essential receptor tyrosine kinase. *Int J Biochem Cell Biol*. 2007;39:1995–1998.

36. Fazel S, Chen L, Weisel RD, Angoulvant D, Seneviratne C, Fazel A, Cheung P, Lam J, Fedak PW, Yau TM, Li RK. Cell transplantation preserves cardiac function after infarction by infarct stabilization: augmentation by stem cell factor. *J Thorac Cardiovasc Surg*. 2005;130:1310.

37. Terrovitis J, Stuber M, Youssef A, Preece S, Leppo M, Kizana E, Schar M, Gerstenblith G, Weiss RG, Marban E, Abraham MR. Magnetic resonance imaging overestimates ferumoxide-labeled stem cell survival after transplantation in the heart. *Circulation*. 2008;117:1555–1562.

CLINICAL PERSPECTIVE

Myocardial infarction (MI) is a major cause of death in coronary heart disease. Loss of myocardium after MI leads to scar formation and subsequent cardiac remodeling characterized by hypertrophy of noninfarct myocardium, left ventricular dilatation, and heart failure. Despite current available treatments, the outcome of MI remains poor. Stem cell factor (SCF) has been shown to promote survival and mobilization of bone marrow stem cells and endothelial progenitor cells. The present study investigated the effects of cardiomyocyte-specific overexpression of the membrane-associated isoform of human SCF (hSCF) on cardiac function after MI. We hypothesized that inducible cardiomyocyte-specific overexpression of membrane-associated hSCF improves cardiac repair, myocardial function, and survival after MI. To test this hypothesis, we generated a novel transgenic mouse that overexpresses membrane-associated hSCF in cardiomyocytes under the control of a Tet-off system. We demonstrated that cardiomyocyte-specific hSCF overexpression increased stem cell and endothelial progenitor cell retention in the infarct myocardium, promoted myocardial angiogenesis, increased capillary density, decreased myocardial apoptosis, and reduced left ventricular hypertrophy after MI. These beneficial effects led to significant improvements in cardiac function and survival in hSCF-overexpressing mice after MI and are likely due to the enhanced recruitment of endothelial progenitor cells to the infarct myocardium and improved cardiac repair. Our study suggests that hSCF may have therapeutic potential in the treatment of heart failure after MI.

SUPPLEMENTAL MATERIAL

Xiang FL, et al.

SUPPLEMENTAL METHODS

Generation of hSCF/tTA Double Transgenic Mice

A new line of tetracycline-inducible cardiac-specific overexpressing membrane associated human stem cell factor (hSCF) mice was generated as previously described.[1] Briefly, membrane-associated hSCF cDNA (accession #: NM_003994) was inserted into the inducible α-myosin heavy chain (MHC) promoter expression vector [1] to permit doxycycline (DOX)-regulated expression in combination with a cardiac-specific tTA-expressing transgene. The fragment containing tetracycline operon, α-MHC promoter and hSCF was injected into the fertilized oocytes, which were then transferred into the oviduct of a pseudo-pregnant female mouse. hSCF transgenic founders were verified by Southern blot analysis. Transgenic line 1 mice were used in the present study. The hSCF mice were crossed with mice created previously that carry a tetracycline-controlled trans-activator (tTA) driven by α-MHC promoter to produce wild type (WT), tTA, hSCF, and hSCF/tTA mice. Genotypes were identified by PCR using genomic DNA from tail biopsies. The following primer pairs were used: tTA, forward, AGC GCA TTA GAG CTG CTT AAT GAG GTC, reverse, GTC GTA ATA ATG GCG GCA TAC TAT C; hSCF, forward, CAA CTG CAG GTC GAC CTG TTT GTG CTG GAT CGC AGC, reverse, CCC AAG CTT GAA GCA AAC ATG AAC TGT TACC. To turn off hSCF expression, the hSCF/tTA mice were treated with 0.2 mg/mL DOX in their drinking water for 2 weeks prior to and continued for 5 or 30 days after sham or MI surgery.

Determination of mRNA Expression by Real-time RT-PCR

Total RNA was extracted from heart tissue using Trizol and cDNA was synthesized using M-MLV reverse transcriptase as previously described.[2] Real-time PCR was conducted using SYBR Green PCR Master Mix as per manufacturer's instructions (Eurogentec, CA). 28S rRNA was used as a loading control. The primer sequences were as follows: hSCF upstream 5'TCA TTC AAG AGC CCA GAA CC3' and downstream 5'CAG ATG CCA CTA CAA AGT CC3'and 28S rRNA upstream 5' TTG AAA ATC CGG GGG AGA G 3' and downstream 5' ACA TTG TTC CAA CAT GCC AG 3'. Samples were amplified for 35 cycles using MJ Research Opticon Real-Time PCR machine. For quantification of the growth factors mRNA level in the heart, the following primer pairs were used: vascular endothelial growth factor (VEGF-A), forward, GAT TGA GAC CCT GGT GGA CAT C, reverse, TCT CCT ATG TGC TGG CTT TGG T; insulin growth factor (IGF-1), forward, CTG CTT GCT CAC CTT CAC CA, reverse, ATG CTG GAG CCA TAG CCT GT; basic fibroblast growth factor (bFGF), forward, CAA GGG AGT GTG TGC CAA CC, reverse, TGC CCA GTT CGT TTC AGT GC; mouse SCF, forward, CGG GAT GGA TGT TTT GCC TA, reverse, CTT CGG TGC GTT TTC TTC CA. The levels of mRNA expression in relation to 28S were determined in the same way as we previously described. [2]

Animal Procedures

Animals in this study were handled in accordance with the *Guide for the Care and Use of Laboratory Animals* published by the US National Institute of Health (NIH publication No. 85-23, revised 1996) and approved by the Animal Use Subcommittee at the University of Western Ontario, Canada. After mice were anaesthetized with an IP injection of ketamine (50 mg/kg) and xylazine (12.5 mg/kg) mixture, myocardium infarction was induced by surgical occlusion of the

left anterior descending coronary artery (LAD) through a left anterolateral approach as we previously described [3]. Both male and female mice at the age between 2-6 months were randomly selected to undergo coronary artery ligation or sham surgery (same procedure without occlusion of the LAD). Investigator was blinded to the genotype of the mice during surgeries. Experiments were performed 5 or 30 days after surgery. Survival was monitored and the left ventricle to body weight ratio was recorded. Infarct size was measured after animals were sacrificed and was expressed as a fraction of the total cross-sectional endocardial circumference of the left ventricle (LV) as we described previously. [3]

Hemodynamic Measurements

Mice were anaesthetized as described in the previous section. A Millar pressure-conductance catheter (Model SPR-839, Size 1.4F) was inserted into the right carotid artery and advanced into the LV. After stabilization for 10 minutes, the signal was recorded continuously and later analysed with a cardiac pressure-volume analysis program (PVAN 3.2; Millar Instruments, TX).[3-5] Mice were then sacrificed and hearts were fixed in 4% paraformaldehyde or stored at -80 °C for further analysis.

Histology

To measure myocytes cell size, cardiac tissue sections were stained with hematoxylin/eosin and photographed by using a digital camera under a microscope (Observer D1, Zeiss) at a magnification of 400x. Myocyte cross sectional diameters at nuclei level [6] were assessed by the AxioVision software. To study stem cell recruitment, tissue sections were stained with rabbit anti-mouse c-kit (1:200, Santa Cruz Biotechnology, CA) and rabbit anti-mouse VEGFR2 primary

antibody (1:200, Abcam, MA) followed by goat anti-rabbit fluorescent secondary antibody. Nuclei were stained with Hoechst 33342. Ten to 15 fields of the peri-infarct area (200-300 μm adjacent to the infarct) were examined for each heart using a fluorescent microscope (Observer D1, Zeiss) at 630x magnification to quantify the c-kit positive and c-kit/VEGFR2 double positive cells. Images were taken using a laser confocal microscope (LSM 510 Meta, Zeiss). To analyze capillary density, tissue sections were stained with biotinylated lectin-I (1:100, Vector Laboratory, CA) followed by Vectastain Elite ABC peroxidise kit with diaminobenzidine tetrahydrochloride (DAB) as a chromogen, and counterstained by hematoxylin. Ten to 14 images were taken in the peri-infarct area of each heart using a digital camera under a microscope (400x, Zeiss). To quantify the mast cells in the heart, cardiac tissue sections were stained with 0.02% toluidine blue in 0.25% acetic acid (pH 2.0-2.5).[7,8] Two to 4 heart sections of each mouse were evaluated.

Caspase-3 Activity and Cytoplasmic Histone-Associated DNA Fragments

Caspase-3 activity and cytoplasmic histone-associated DNA fragments were measured using caspase-3 cellular activity assay kit (BIOMOL, Plymouth Meeting, PA) and cell death detection ELISA (Roche, Mississauga, ON), respectively as we previously described.[9]

***In vivo* Matrigel Angiogenesis**

In vivo angiogenesis was assessed by myocardial matrigel implantation as described.[10] Three days after matrigel implantation, heart tissue were collected and embedded in paraffin. Sections were cut and stained with hematoxylin and eosin. Results are expressed as the percentage of the vessel-like area to the total matrigel area.

Statistical Analysis

Data are expressed as the mean ± SEM. One- or two-way ANOVA followed by Bonferroni test was performed for multiple group comparisons. Unpaired Student's t test was used between two groups. Kaplan and Meier survival curves were analyzed by Log-rank (Mantel-Cox) test. Differences were considered significant at the level of $P<0.05$.

SUPPLEMENTAL TABLES

Table S1. Number of mast cells in the left ventricular myocardium 5 and 30 days after sham or MI surgeries.

Groups		Sub-epicardium	Non-infarct	Peri-infarct
5-day sham	WT	1.7±0.8	3.1±1.0	-
	hSCF/tTA	2±1.1	2.6±1.2	-
5-day MI	WT	2.3±1.0	0.4±0.2	1.4±0.3
	hSCF/tTA	0.7±0.4	0.2±0.2	0.9±0.4
30-day sham	WT	1.4±0.4	1.9±0.8	-
	hSCF/tTA	0.9±0.9	1.0±0.7	-
30-day MI	WT	2.3±0.9	1.1±0.8	0.6±0.2
	hSCF/tTA	2.3±0.1	0.0±0.0	0.7±0.5

Data are mean ± SEM of mast cells per heart section from 4 animals per group. Two-way ANOVA followed by Bonferroni test. There was no statistical difference between any groups.

SUPPLEMENTAL FIGURES

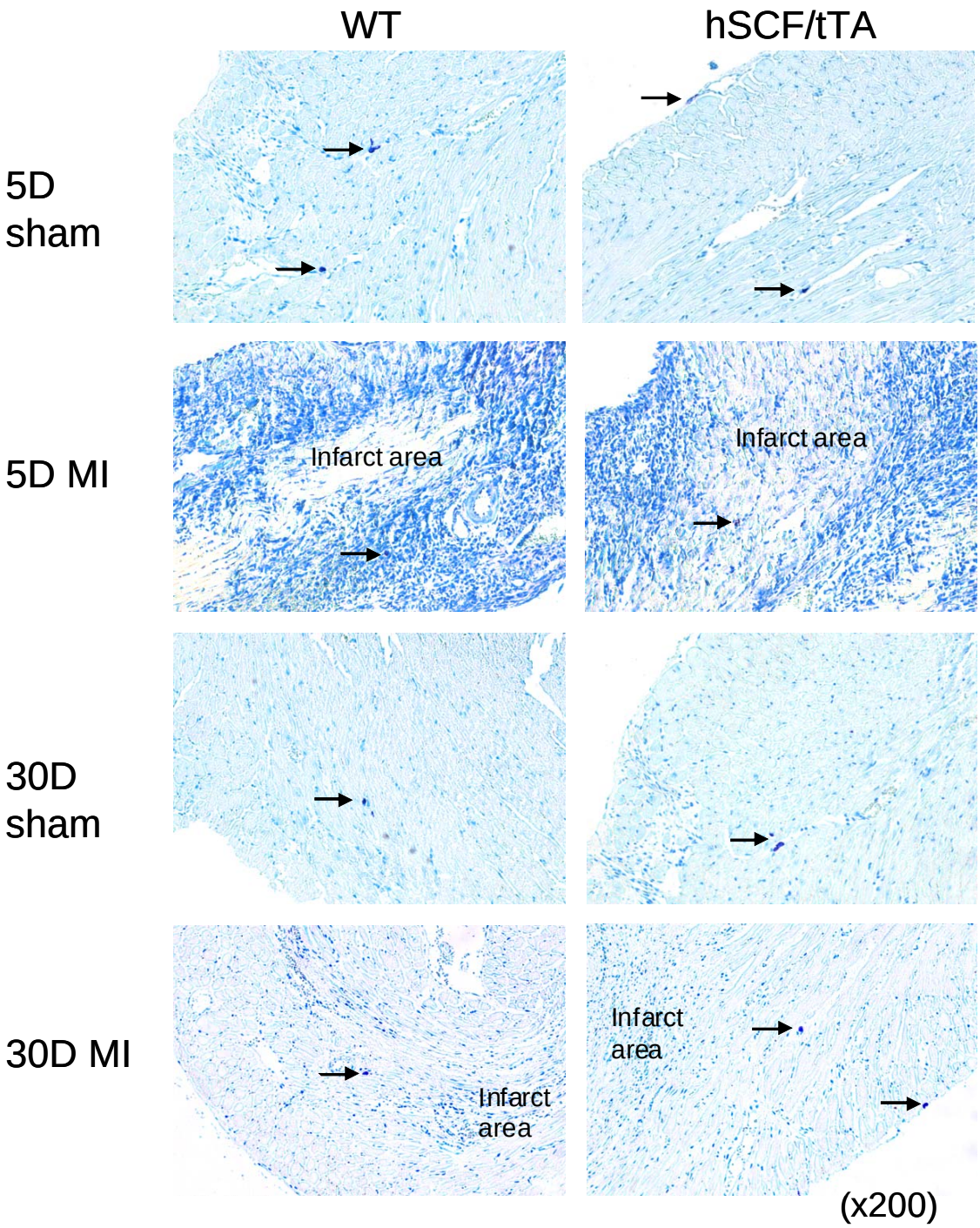

Figure S1

FIGURE LEGENDS

Figure S1. Mast cell staining using toluidine blue in heart tissue sections from WT and hSCF/tTA mice. Mice were subjected to sham or myocardial infarction (MI) for 5 or 30 days. Arrows indicate mast cells. Infarct area is labeled.

SUPPLEMENTAL REFERENCES

1. Sanbe A, Gulick J, Hanks MC, Liang Q, Osinska H, Robbins J. Reengineering inducible cardiac-specific transgenesis with an attenuated myosin heavy chain promoter. *Circ Res*. 2003;92:609-616.
2. Hammoud L, Xiang F, Lu X, Brunner F, Leco K, Feng Q. Endothelial nitric oxide synthase promotes neonatal cardiomyocyte proliferation by inhibiting tissue inhibitor of metalloproteinase-3 expression. *Cardiovasc Res*. 2007;75:359-368.
3. Feng Q, Lu X, Jones DL, Shen J, Arnold JMO. Increased inducible nitric oxide synthase expression contributes to myocardial dysfunction and higher mortality post-myocardial infarction in mice. *Circulation*. 2001;104:700-704.
4. Detombe SA, Ford NL, Xiang F, Lu X, Feng Q, Drangova M. Longitudinal follow-up of cardiac structure and functional changes in an infarct mouse model using retrospectively gated micro-computed tomography. *Invest Radiol*. 2008;43:520-529.
5. Peng T, Zhang T, Lu X, Feng Q. JNK1/c-fos inhibits cardiomyocyte TNF-alpha expression via a negative crosstalk with ERK and p38 MAPK in endotoxaemia. *Cardiovasc Res*. 2009;81:733-41.
6. Scherrer-Crosbie M, Ullrich R, Bloch KD, Nakajima H, Nasseri B, Aretz HT, Lindsey

ML, Vancon AC, Huang PL, Lee RT, Zapol WM, Picard MH. Endothelial nitric oxide synthase limits left ventricular remodeling after myocardial infarction in mice. *Circulation*. 2001;104:1286-91.

7. Blumenkrantz N, Asboe-Hansen G. A selective stain for mast cells. *Histochem J*. 1975;7:277-82.

8. Dewald O, Ren G, Duerr GD, Zoerlein M, Klemm C, Gersch C, Tincey S, Michael LH, Entman ML, Frangogiannis NG. Of mice and dogs: species-specific differences in the inflammatory response following myocardial infarction. *Am J Pathol*. 2004;164:665-77.

9. Feng Q, Song W, Lu X, Hamilton JA, Lei M, Peng T, Yee SP. Development of heart failure and congenital septal defects in mice lacking endothelial nitric oxide synthase. *Circulation*. 2002;106:873-879.

10. Zhao X, Lu X, Feng Q. Deficiency in endothelial nitric oxide synthase impairs myocardial angiogenesis. *Am J Physiol Heart Circ Physiol*. 2002;283:H2371-H2378.